Chapter 1
Fundamental of $CuGaSe_2$

Semiconducting solar cell based materials such as I-III-VI_2 chalcopyrites can be tuned by the elemental composition for optimum device performance. Among all known thin film solar cells, photovoltaic devices based on these materials have reached the highest efficiencies and continue to advance towards economic viability. In this chapter the so far well known properties of the $CuGaSe_2$ chalcopyrites semiconductors are reviewed. The need of chalcopyrites for solar cells is presented in the section 1.1. We briefly describe how relevant $CuGaSe_2$ compounds are as function absorber material for solar cell applications. In the second section 1.2, we give a background of chalcopyrite structure including crystal structure, phase diagram and band structure. Section 1.3 provides the basis of $CuGaSe_2$ optical and electrical properties and also addresses some difficulties encountered when they are be doped.

1.1 Relevance of chalcopyrites thin films for solar cells

Ternary I-III-VI_2 compound semiconductors, specially $CuGaSe_2$ have attracted considerable scientific interest as absorber material for photovoltaic device due to their:

- Very high optical absorption coefficient for visible light ($\alpha \backsim 10^4$ cm^{-1}). Most of the incoming photons with energy greater than 1.68 eV are absorbed within the first micrometers of the materials [4].
- Favorable direct wide band gap (1.68 eV at room temperature), which matches the optimum value for terrestrial applications of 1.5 eV, and permits a large absorption of the solar spectrum. This makes them well suited for efficient conversion of solar light into electricity [5]
- Interesting defect physics, namely the ability to form electronically inactive defect complexes, leading to a great tolerance of these compounds to foreign impurities and deviations from the ideal stoichiometry [4].
- Outstanding radiation hardness that makes them suitable for space applications[6].
- Predicted high theoretical efficiencies ($> 25\%$) for single junction cells (figure 1.1) calculated from basic semiconductor equations [7].

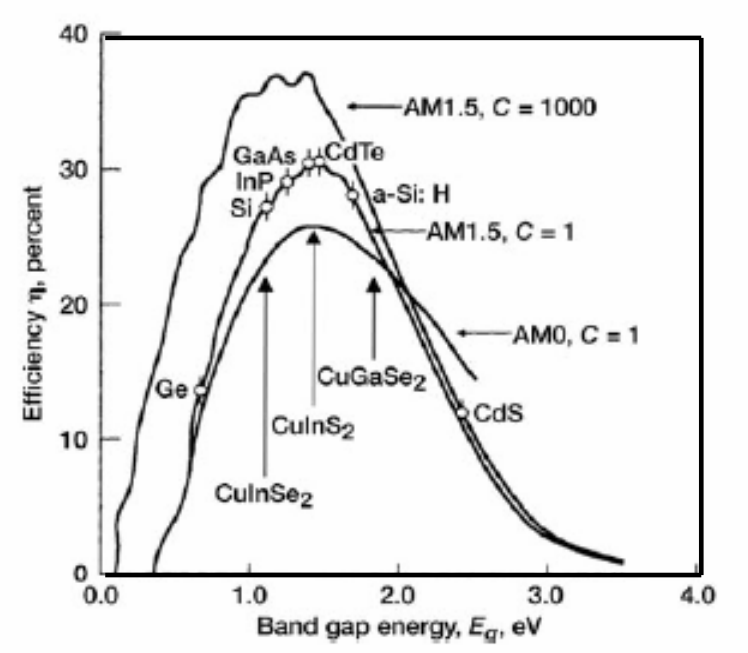

Figure 1.1. *Theoretical predicted efficiency versus bandgap for thin-film photovoltaic materials for solar spectra in space (AM 0) and on the surface of the Earth (AM 1.5) at 300K compared with bandgaps of other PV materials with unconcentrated (C = 1) and high concentration (C = 1000) sunlight* [8].

- Highly achieved efficiencies solar cell devices on the laboratory scale as reviewed in table 1.1.

Table 1.1: *Efficiencies of laboratory scale solar cells devices based on I-III-VI_2 materials.*

Device	Efficiency η [%]	Reference
$CdS/ZnO/CuGaSe_2$	10.2	AbuShama *et al*, 2005 [10]
$CdS/ZnO/Cu(In,Ga)Se_2$	19.5	AbuShama *et al*, 2005 [11]
$CdS/ZnO/CuInSe_2$	15	AbuShama *et al.*, 2005 [10]
$CdS/ZnO/CuInS_2$	11.4	Siemer *et al.*, 2001[12]

- A large variety of available growth processes for the fabrication of good device quality $CuGaSe_2$ thin films.[13].

1.2 Structural properties of $CuGaSe_2$.

1.2.1 Chemical structure of $CuGaSe_2$ chalcopyrite compound

The mineral chalcopyrite $CuFeS_2$ is a common and well known mineral. The crystal structure of chalcopyrite was first determined by Burdick and Ellis [15]; it has a structure of an ordered arrangement of Cu and Fe ions within the double sphalerite (ZnS) unit cell [16].

The chalcopyrite structures are derived from their isoelectric binary II-VI zinc blende (ZB) structural analogons [14]. Pure chalcopyrites are ternary semiconducting compounds with the chemical formula such as $CuGaSe_2$, where Cu, Ga, and Se represent respectively elements from groups I, III, and VI of the periodic table. The group-II atoms in the binary ZB compound can be alternately replaced by elements from group I and III. For example $CuGaSe_2$ is derived from the ZB structure of II-VI compounds like ZnSe by occupying the Zn sites alternately with Ga and Cu atoms as shown in the equation 1.1:

$$\mathrm{ZnSe} \equiv \mathrm{Zn_2Se_2} \xrightarrow[\mathrm{Zn \longrightarrow Ga}]{\mathrm{Zn \longrightarrow Cu}} \mathrm{CuGaSe_2} \tag{1.1}$$

A schematic representation of the ideal $CuGaSe_2$ chalcopyrite structure derived from ZnSe zinc-blende crystal is shown in figure 1.2, with a doubling in the c direction rather than one as in the ZB compounds, and two different cations, Cu and Ga. In the chalcopyrite structures, the lattice elements are tetrahedrally coordinated as in diamond- like semiconductors, where each Cu or Ga atom is coordinated to Se atoms, whereas each Se atom has two bonds to Cu and two to Ga atoms. Due to the presence of two different cations, Cu and Ga, instead of one cation as in zinc blende compounds, the properties of chalcopyrites differs from those of their isoelectric zinc blende analogons and the chalcopyrite structure can be seen as a superlattice of the zinc- blende structure.

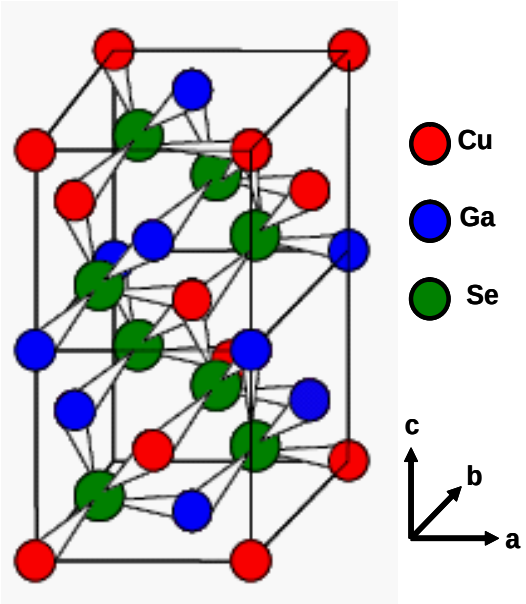

Figure 1.2: *Unit cell of $CuGaSe_2$ chalcopyrite structure in the tetragonal D_{2d}^{12} space group. The a and b directions are equivalent ($a = b = 0.5619$) and the c axis is different ($c = 1.1026$).*

To sum up; chalcopyrite structure has a tetragonal unit cell with two lattice parameters a and c, in the ratio of $c/a = 1.962$ [17], and belongs to the space group D_{2d}^{12} with eight atoms

per primitive unit cell, which is a superlattice of ZB structure with two atoms per primitive unit cell. The precise location of Se atoms in the chalcopyrite structure depends on the strength of Cu-Se and Ga-Se bonds. A stronger bonding of Se atoms with the two nearest Cu- atoms was suggested by Robbins *et al* [18], presumably due to the d-electrons of the Cu- atom contribution to the bonding, leading to a difference of the strengths of the Cu-Se and Ga-Se bonds; therefore the Cu-Se and Ga-Se bond lengths, labelled d_{Cu-Se} and d_{Ga-Se} are different. The consequences of having unequal anion cation bond lengths are:

- The tetragonal distortion which describes the new position of anions. Indeed, the lattice constant ratio c/a found in the chalcopyrite structure in general deviates from that of the ideal value 2 and is 1.96 for $CuGaSe_2$. The deformation of the unit cell to a length c which is different from $2a$ is characterized by the tetragonal distortion given by $\eta = c/2a$ and differs therefore from one [19].
- The Se anions are displaced from their ideal positions by an amount u (equation 1.2) known as a free parameter of the chalcopyrite structure, which describes the reposition of the anions in the (x, y) plane.

$$u = \frac{1}{4} + \frac{\left(d^2_{Cu-Se} - d^2_{Ga-Se}\right)}{a^2} \tag{1.2}$$

1.2.2 Phase diagram of $CuGaSe_2$

A phase can be defined as a state having a particular composition and also definite characteristic crystal structure [20]. A phase can be in solid, liquid or gas form and there may exist more than one distinct crystalline phase. The understanding of the phase formation of ternary $CuGaSe_2$ compounds and their phase equilibria is discussed in terms of temperature and composition. It shows, how much stoichiometric deviation in $CuGaSe_2$ can be tolerated, without forming foreign phases. Figure 1.3 displays a pseudobinary cut of the Cu - Ga - Se phase diagram between $(Cu_2Se)_{1-x}$ and $(Ga_2Se_3)_x$ [21]. In the case of Cu-based chalcopyrites, the formation of copper selenides for small deviations form the 1-1-2-stoichiometry or even stoichiometric compositions are predicted by the phase diagram.

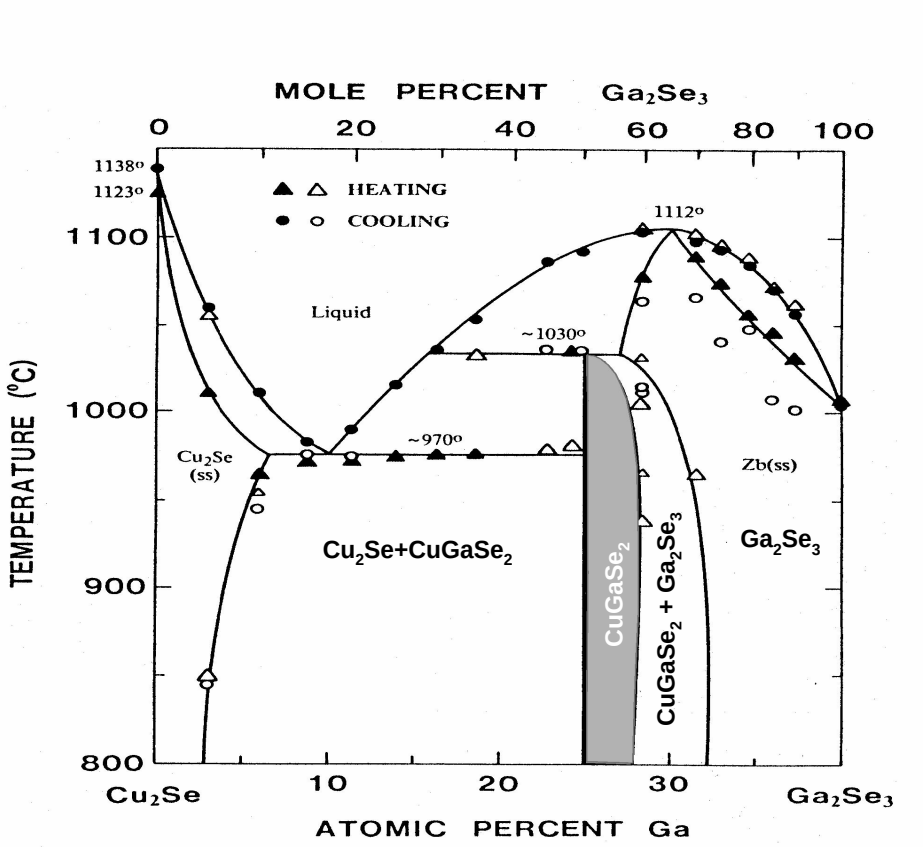

Figure 1.3. *Cu_2Se - Ga_2Se_3 pseudobinary diagram for temperatures $T > 800$ °C at 1 atm.* [21]

Structural, optical and electronic properties of chalcopyrite thin films depend on the presence of secondary phases in the material. Because the presence of either Cu-rich or Ga-rich secondary binary phases in $CuGaSe_2$ hampers the device performance, phase diagrams are useful to firstly predict the occurrence of these phases and secondly eliminate them. According to the phase diagram in figure 1.3, where the transition temperatures as a function of composition are displayed in the range from 0 to 50 mol % Ga_2Se_3, various compounds can occur in the $CuGaSe_2$ ternary systems. $CuGaSe_2$ chalcopyrite structure is stable in the temperature range of 800° C - 1150° C. The $CuGaSe_2$ single phase extends from the stoichiometric of 25 at% Ga_2Se_3 to the Ga-rich composition of about 28 at% Ga_2Se_3. The corresponding Ga/Cu ratio for the singe phase lies between 1.0 and 1.38. In the case where the Ga/Cu atomic ratios are less than 1.0, mixtures of $CuGaSe_2$ $+(Cu_2Se)_{1-x}$ are predicted, while for Ga/Cu greater than 1.38, the materials are expected to contain secondary phases of the type $CuGa_3Se_5$ and $CuGa_5Se_8$. The pseudobinary cut points out the great structural tolerance of the $CuGaSe_2$ compound, up to 10 mol% deviations from the stoichiometry towards the Ga_2Se_3 side.

1.2.3 Electronic band structure of $CuGaSe_2$

Due to the fact that in both the chalcopyrite materials and their binary zinc blende (ZB) analogons the chemical binding occurs through hybrid sp^3-orbitals, the band structure of ternary chalcopyrites can be derived form that of their ZB analogons. Ternary chalcopyrite $CuGaSe_2$ conduction band is built by s-like states having the symmetry Γ, whereas the valence band maximum is a p-like state. However, the uppermost valence bands of chalcopyrite are influenced by the vicinity of the noble metal d-levels as confirmed by electroreflectance studies [23]. The valence band is split into three bands E_1, E_2, E_3, due to the influence of spin-orbit interaction Δ_{so} and crystal field Δ_{cf} in the tetragonal structure. The optical transitions between these three valence sub-band maxima and the conduction band minimum are generally labeled by $E_0(A)$ (refers to heavy hole), $E_0(B)$ (refers to light hole) and $E_0(C)$ (refers to crystal-field split band).

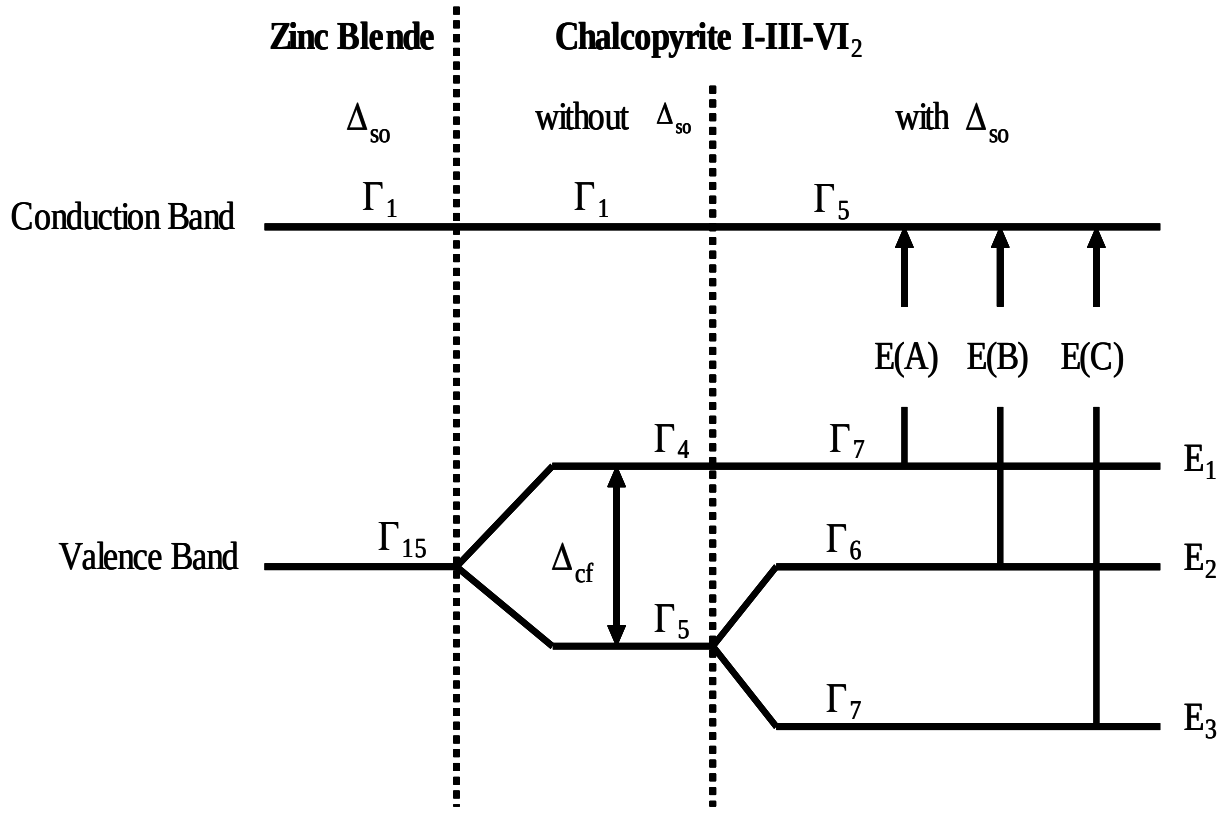

Figure 1.4. *Schematic band structure and selection rules for the zinc blende (ZB) and chalcopyrite structures showing crystal field and spin-orbit splitting of the valence band. Three different bandgaps ($E_0(A)$, $E_0(B)$, $E_0(C)$) are shown.* (from [25]).

Figure 1.4 depicts the band diagram for the chalcopyrite $CuGaSe_2$ structures. The experimental values of the three energies in the $CuGaSe_2$ crystal with their corresponding spin-orbit interaction Δ_{so} and crystal field Δ_{cf} are summarized in table 1.2

Table 1.2: *Experimental values of the three energies $E_0(A)$, $E_0(B)$, $E_0(C)$ in $CuGaSe_2$ crystal at Γ point with their corresponding spin-orbit interaction $\Delta_{\rm so}$ and crystal field $\Delta_{\rm cf}$.*

$E_0(A)$ [eV]	$E_0(B)$ [eV]	$E_0(C)$ [eV]	$\Delta_{\rm so}$ [eV]	$\Delta_{\rm cf}$ [eV]	T [K]	Reference
1.729	1.813	2.016	0.23	-0.11	77	[26]
1.721	1.806	2.012	0.23	-0.11	77	[27]
1.68	1.75	1.96	0.23	-0.09	300	[13]

The interaction between the Γ_1 and Γ_{15} levels in chalcopyrite materials raises the uppermost Γ_{15} level to higher energies. Hence, the direct band gap of chalcopyrite at the Γ- point is generally lower than that of their corresponding binary analogs. For example the band gap difference between $CuGaSe_2$ compound and its binary ZnSe analogon is $E_g^{ZnSe} - E_g^{Cu\,GaSe_2} = 1.eV$. This effect known as "band gap anomaly", ΔE_G have been explained by Jaffe *et al* [14] the shift in the band to smaller values for ternary compounds in terms of a structural factor, ΔE_G^S , and a chemical factor , ΔE_G^{Chem}. In the former case, the uppermost valence band is elevated due to the simultaneous influence of crystal field $\Delta_{\rm cf}$ interaction resulting from the uniaxial tetragonal distortion of the crystal lattice (c/a) and the displacement of group VI anions from the ideal position, and the spin orbit interaction $\Delta_{\rm so}$. In the latter, the $4d$ or $3d$ electrons of the metal hybridize with the p-like valence band (p-d hybridization) due the vicinity of their levels, resulting in a shrinkage of the band gap by up to 1eV. Therefore, taking into account both these effects, in comparison to their binary analogs, the band gap of chalcopyrites is much smaller and shifts to lower energies. This modification in the energy band structure is also explained by the fact that valence bands of zinc-blende material are composed of s and p -like orbitals, whereas the metal d-levels of chalcopyrites hybridize with the s and p -like orbitals.

It is well established that $CuGaSe_2$ has a direct band gap of 1.68 eV at 300K and the variation of the band gap of chalcopyrite compounds with temperature is anomalous compared to their binary analogons. Studies on $CuGaSe_2$ single crystals and thin films have shown that the energy gap decreases with increasing temperatures as does its binary analogs, and can be described approximately by the relation proposed by Varshni's empirical equation [28] for temperatures T < 100K:

$$\Delta E_0(T) = E_G(0) - E_G(T) = \alpha T^2/(T+\beta) \tag{1.3}$$

where $E_G(T)$ is the band gap, $E_G(0)$ is its value at 0 K and β is a parameter of the same order as the Debye temperature θ_d, which describes and α is given by $-\frac{dE_G(T)}{dT}\,|_{T\longrightarrow\infty}$

1.3 Electrical and optical properties of $CuGaSe_2$ based devices

In this section we review the general model for defects encountered in the $CuGaSe_2$ compounds in combination with the predictions of theoretical calculations, and how these defects affect the main properties of $CuGaSe_2$ material.

1.3.1 Crystal defects $CuGaSe_2$

Optical and electrical properties of $CuGaSe_2$ are essentially affected by defects and point defects. Defects are defined as imperfections in a perfect crystal lattice, while point defects are dimensionless defects involving single atoms or complexes of few atoms. Among the well known defects are vacancies (missing atoms from the lattice), substitutions (atoms on another lattice element) and interstitials (extra atom between normal lattice sites). Besides these above cited defects, one-dimensional defects involving a line of continuous defects (dislocations), two-dimensional defects including (Grain boundaries, twin boundaries, interfaces, stacking faults) and three-dimensional bulk defects (voids of point defects) can be cited. $CuGaSe_2$ is a complex semiconductor material with high concentration of defects [29] that involves 12 intrinsic defects, namely 3 vacancies (V_{Cu}, V_{Ga}, V_{Se}), 3 interstitials (Cu_i, Ga_i, Se_i) and 6 antisites (Cu_{Ga}, Cu_{Se}, Ga_{Cu}, Ga_{Se}, Se_{Cu}, Se_{Ga}). According to the theoretical calculation of the formation energies with first-principles self consistent electronic structure performed by Neumann [30], Ga_i, Ga_{Cu}, Se_{Cu}, and Se_{Ga} act as donors, whereas V_{Cu}, V_{Ga}, Se_i, Cu_{Ga}, Cu_{Se} act as acceptors. Selenium vacancies V_{Se} were described as having either donor or acceptor behavior (amphoteric behavior) [31].

1.3.2 Models for defect structures

Based on calculations with first-principles self consistent electronic structure theory, Zhang *et al* [32] have calculated the electronic structure and the formation energies of metal related point defects in $CuGaSe_2$ and its alloys by using local density approximation and the first principles linearized augmented plane wave pseudopotentential technique together with the supercell approximation. According to these calculations, is was shown that:

- The defect formation energy of defects is not always constant but depends on the electrochemical potential of the electrons (Fermi level E_F). For a point defect α in a charge state q the defect formation energy is from [32]:

$$\Delta H(\alpha, q) = Cte + qE_F \tag{1.4}$$

where the constant term depends on the chemical potential of particular atomic species during film growth but not on the Fermi energy [35].

- The defect concentration in a crystal depends on its formation energy, ΔH, following this form:

$$C = N_{sites}\exp\left(-\frac{\Delta H}{k_B T}\right) \tag{1.5}$$

where N_{sites} is the concentration of sites in the crystal where the defects can occur.

From equation 1.5 one notes that the higher the equilibrium concentration of the defect is, the lower its formation energy. A high formation energy means that defects are unlikely to form. For specific atom species, the defect formation energy as well as the chemical potential vary with the Fermi level.

Table 1.3: *Theoretical computed enthalpies and ionization energies of intrinsic defects and their assignment in $CuGaSe_2$* [30, 36]

Defect	defect nature	Ionization Energy [meV]	Defect formation energy [eV]
V_{Cu}	Acceptor	10	0.67
V_{Ga}	Acceptor	190	2.83
V_{Se}	Donor	-	2.30
Cu_{Ga}	Acceptor	290	1.41
Ga_{cu}	Donor	490	4.22
Ga_{int}	Donor	-	-
Cu_i	Donor	210	1.91

Table 1.3 summarizes the calculation of the defect formation energy and the defect ionization energies. A low formation energy defect such as V_{Cu} in Cu-chalcopyrite would imply the spontaneous formation of large numbers of those defects if the Fermi level changes. In contrast, Se-site occupation with one of the metal atoms is unlikely to occur due to their high formation energy, and they are not listed in table 1.3. The preferential formation of electrical neutral defect- pairs complexes consisting of charged defects such as: ($2Cu_i^+$, Cu_{Ga}^{2-}), (Cu_{Ga}^{2-}, Ga_{Cu}^{2+}) and ($2V_{Cu}^-$, Ga_{Cu}^{2+}), with formation energies lower than those of their corresponding isolated defects by intrinsic defects was also highlighted by Zhang *et al* [32]. For example the defect pair ($2V_{Cu}^-$, Ga_{Cu}^{2+}) shown in figure 1.5 is a deep recombination center that was found not to significantly influence the electrical performance of the material and not to exhibit any electronic transition within the band gap. In contrast, the isolated cation vacancy V_{cu} and isolated cation antisite Ga_{Cu} act as an acceptor and donor respectively. The formation of the defect- pair, ($2V_{Cu}^-$, Ga_{Cu}^{2+}), via periodic repetition gives rise to the appearance of secondary phases such as ordered vacancies compounds (OVC) following the equation 1.6:

$$CuGaSe_2 + n\left[2V_{Cu}^- + Ga_{Cu}^{2+}\right]^{\circ} \Longrightarrow Cu_1Ga_3Se_5 \text{ or } Cu_1Ga_5Se_8 \tag{1.6}$$

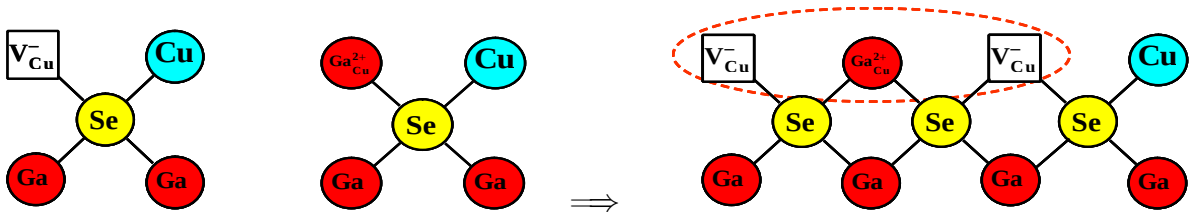

Cation vacancy *Cation antisite* *Neutral* $\left[2V^-_{Cu} + Ga^{2+}_{Cu}\right]$ *complex*

Figure 1.5: *The formation the of the* $(2V^-_{Cu}, Ga^{2+}_{Cu})$ *defects in chalcopyrites compounds.*

1.3.3 Doping of $CuGaSe_2$

According to basic principles underlying the formation energy of various intrinsic defects in common photovoltaic materials, the doping of semiconductors is limited. Although chalcopyrite structures exhibit many similarities in their properties with their zinc blende analogons, there exits a huge difference in their dopability. For example while ZnSe compounds, an isolectric binary of $CuGaSe_2$, have been reported to show both p and n-type behavior, $CuGaSe_2$ have been reported to be of p-type irrespective of their compositions [33]. In the latter case this hurdle has been lifted and the n-type $CuGaSe_2$ was realized by ion implantation of Ge subsequently followed by annealing in Zn atmosphere to remove the compensation [37]. The doping behavior of chalcopyrite compounds has been predicted by the phenomenological "doping pinning rule" developed by Zhang *et al* [38]. Accordingly, $CuGaSe_2$ is predicted to be p-type for all the compositions whereas both n-type and p-type can be achieved in ZnSe. The "doping limit rule" reads:
For n-type doping: "A material cannot be doped successfully n-type if its conduction band minimum (CBM) is close to the vacuum level (i.e. electron affinity is too small)" this is the case for $CuGaSe_2$ where negatively charged defects such as cation-vacancies will form and then compensate the electron supplying agent defect such as Ga^{2+}_{Cu}. In order to increase the n-type dopability, one has to lower the CBM.
Conversely for p-type doping: "A material cannot be doped successfully p-type if its valence band minimum (VBM) is too far from the vacuum level (i.e. intrinsic work-function is too big)". By adding a d-band metal like Cu, one can enhance the p-type dopability because the d-states repel upwards the anion p-states that form the VBM.

1.3.4 Compensation and potential fluctuations:

The electrical compensation is the balance or equilibrium electron donating or accepting point defects. This temporarily removes both the effect of acceptors and donors from acting on the material. The simplest case of compensation involves a transition of an electron from a shallow donating defect state to a shallow accepting defect state, and more complicated compensation involves both shallow acceptors or donors, and deep states. If the concentrations of donor and acceptor defect states are in balance, then the semiconductor is compensated and its doping concentration fulfills the conditions: $n.a_e^3 \ll 1$ or $p.a_h^3 \ll 1$ [39],

where n and p are the concentration of electrons and holes respectively, a_e and a_h are the Bohr radius of the electron and holes respectively.
Potential fluctuations are chiefly encountered in compensated semiconductors, such as Cu-deficient $CuGaSe_2$ chalcopyrite compounds. During potential fluctuations, a captured carrier at an impurity site can not only have direct recombination with a carrier of the opposite type, but can also, prior to recombination, transfer to a state lower in energy leading to a lower energy photon. In the highly compensated material, charged acceptors and donors lead to a random distribution of spatially separated potential wells in both the impurity and band states, where the fluctuations in the ionized impurity concentrations leads to potential fluctuations and gives rise to a broad band of states, which in turn prompts band bending as schematically depicted in figure 1.6.

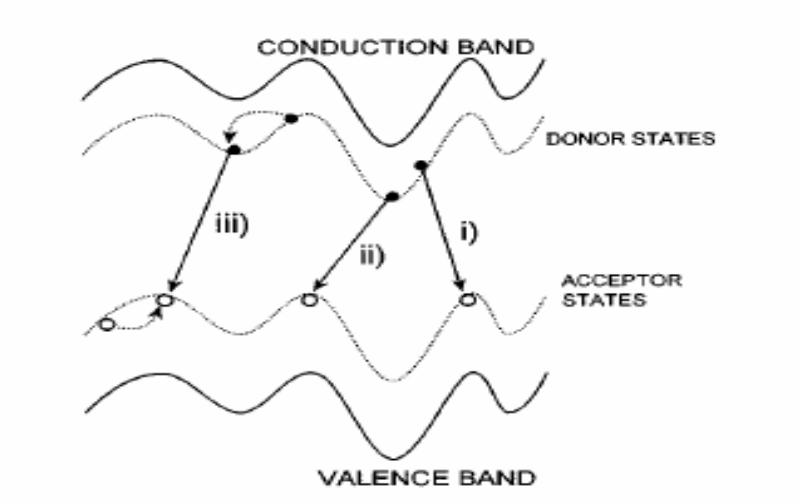

Figure 1.6: *Schematic representation of the perturbed band and impurity states in the presence of potential fluctuations. An electron captured at a donor defect state tends to recombine with holes at the closest neutral acceptor states giving rise to direct transitions i) and ii). The carriers, prior to recombination could also tunnel to the closest well by indirect recombination with lower photon energy emission, thus reducing the energy of the transition iii).*